

# QPatch HTX: Biophysical and pharmacological characterization of ligand-gated ion channels in multi-hole mode

全自動パッチクランプシステム、QPatch HTX、におけるマルチホールテクノロジーを用いたリガンド作動性イオンチャネルに関する生物物理学および薬理学的基礎検討

SOPHION BIOSCIENCE, INC.  
Technology Centre of New Jersey  
675 US Highway One,  
North Brunswick, NJ 08902  
UNITED STATES

SOPHION BIOSCIENCE K.  
IOC Honjo Waseda #V203  
1011, Nishitomida  
Honjo-shi,  
Saitama 367-0035  
JAPAN

SOPHION BIOSCIENCE A/S  
Baltorpvej 154  
DK - 2750 Ballerup  
DENMARK  
info@sophion.com - www.sophion.com



KEITA TAKEUCHI M. KNIRKE JENSEN RIKKE L SCHRØDER HERVØR L OLSEN RASMUS B JACOBSEN JEFFREY WEBBER MATS HOLMQVIST SØREN FRIIS DORTHE NIELSEN METTE T CHRISTENSEN MORTEN SUNESEN

## Introduction

The multi-hole patch clamp technology for the QPatch enables gigaseal recordings of up to ten cells patch-clamped on a single measurement site. In this set of experiments, we have convincingly demonstrated that multi-hole QPatch experiments of fast and slow desensitizing ligand-gated ion channels perform as well as single-hole QPatch experiments with respect to both biophysical and pharmacological characteristics.

In the QPlate X, the ten patch holes have a relatively wide spatial distribution to avoid intercellular contact and downstream space clamp issues. The wide spatial distribution could, on the other hand, potentially slow down the liquid exchange times. We examined the glutamate receptor GluR5, the nicotinic acetylcholine receptor nAChR  $\alpha 1$ , the acid-sensing ion channel ASIC1a, and the anionic  $\gamma$ -aminobutyric acid receptor A GABA-A  $\alpha 1\beta 2\gamma 2$  with regards to agonist rise-time, reversal potential and pharmacological properties on the QPatch HTX in multi-hole mode and compared to results obtained in the classic single-hole mode. All data clearly demonstrate that while the amplitude of the elicited ion channel current is multiplied by a factor of 7-10, and the success rate in terms of usable current amplitude is increased, other significant biophysical properties of these ion channels remain unaltered.

## Material and Methods

### QPatch Experiments:

**Cells:** TE671-nAChR $\alpha 1$  (endogenously expressed), HEK-GABA-A  $\alpha 1\beta 2\gamma 2$ , HEK-ASIC1a, HEK-GluR5. All cells were grown according to their respective SOPs as developed by Sophion Bioscience. Cells were kept in a serum-free medium in the on-board cell hotel on the QPatch and used up to 5 h after harvest.

**Saline solutions:** Extracellular saline (in mM): CaCl<sub>2</sub> 2, MgCl<sub>2</sub> 1, HEPES 10, KCl 4, NaCl 145, glucose 10. pH 7.4, 300 mOsm. Intracellular saline ASIC1a (in mM): CsF 135, EGTA/CsOH 1/5, HEPES 10, NaCl 10. pH 7.3, 290 mOsm. Intracellular saline other ion channels (in mM): KF 120, KCl 20, HEPES 10, EGTA 10. pH 7.2, 290 mOsm.

**QPatch experiments:** All experiments were carried out with the QPatch 16X or QPatch HTX, which performs 16 or 48 parallel and independent patch-clamp recordings on a disposable QPlate with a single patch hole per measurement site, or QPlate X with 10 holes per measurement site.

Figure 1.

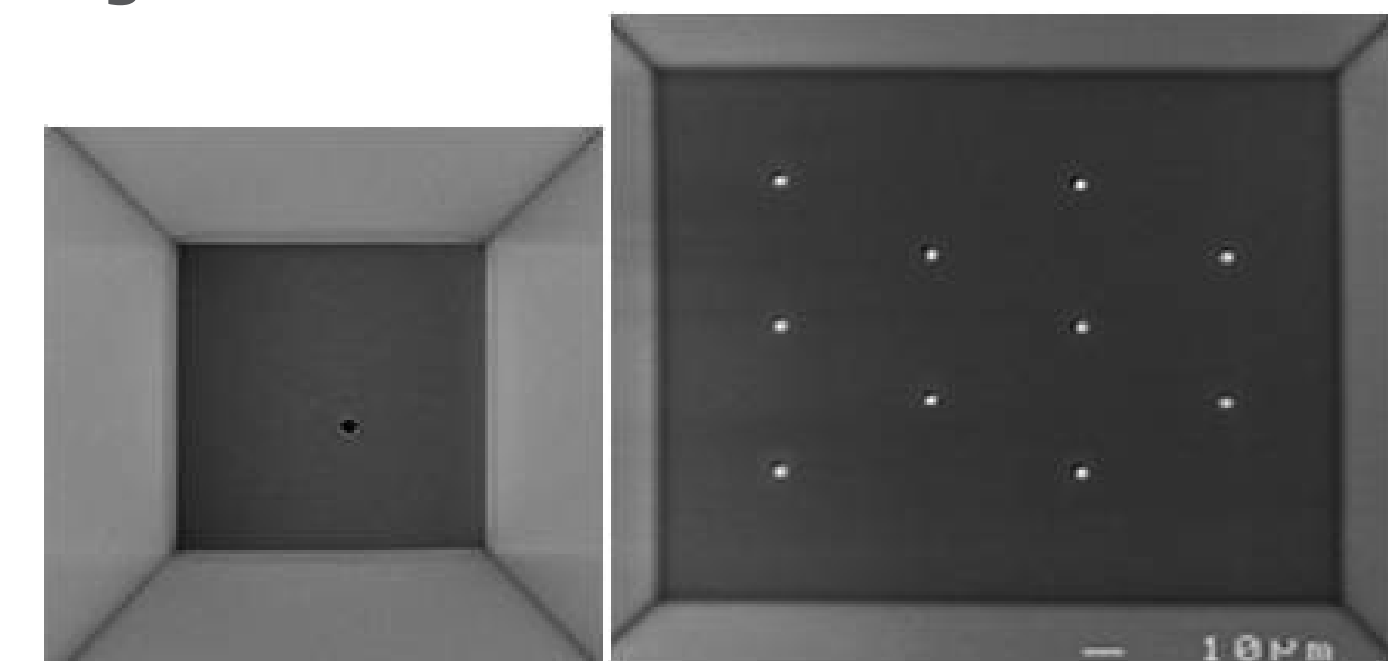


Figure 1. Left: single-hole silicon chip in the QPlate. Right: multi-hole in the QPlate

Positioning of the cells on the measurement site in the QPlate was done by application of negative hydrostatic pressure. Gigaseal and whole-cell configurations were achieved using suction pulses according to the settings specified in the assay optimized for the individual cell lines.

## References:

- Paul M, Kindler CH, Fokt RM, Dresser MJ, Dipps NCJ, Yost CS, Anesth. Analg., 2002;94:597-603  
Shao Z, Mellor IR, Brierley MJ, Harris J, Usherwood PNR, J. Pharm. Exp. Ther. 286:1269-1276, 1998  
Li A, Si W, Hu XW, Liu CJ, Cao XH, Neurosci Bull. 2008 Jun; 24(3):160-5  
Lerma J, Paternain AV, Rodriguez-Moreno A, Lopez-Garcia JC, Physiol. Rev. 2001 Jul;81(3):971-98  
Paternain AV, Vicente A, Nielsen EO, Lerma J, Eur J Neurosci. 1996 Oct;8(10):2129-36  
Feigenspan A, Weiler R. Electrophysiological properties of mouse horizontal cell GABA receptors. J Neurophysiol. 2004 Nov;92(5):2789-801

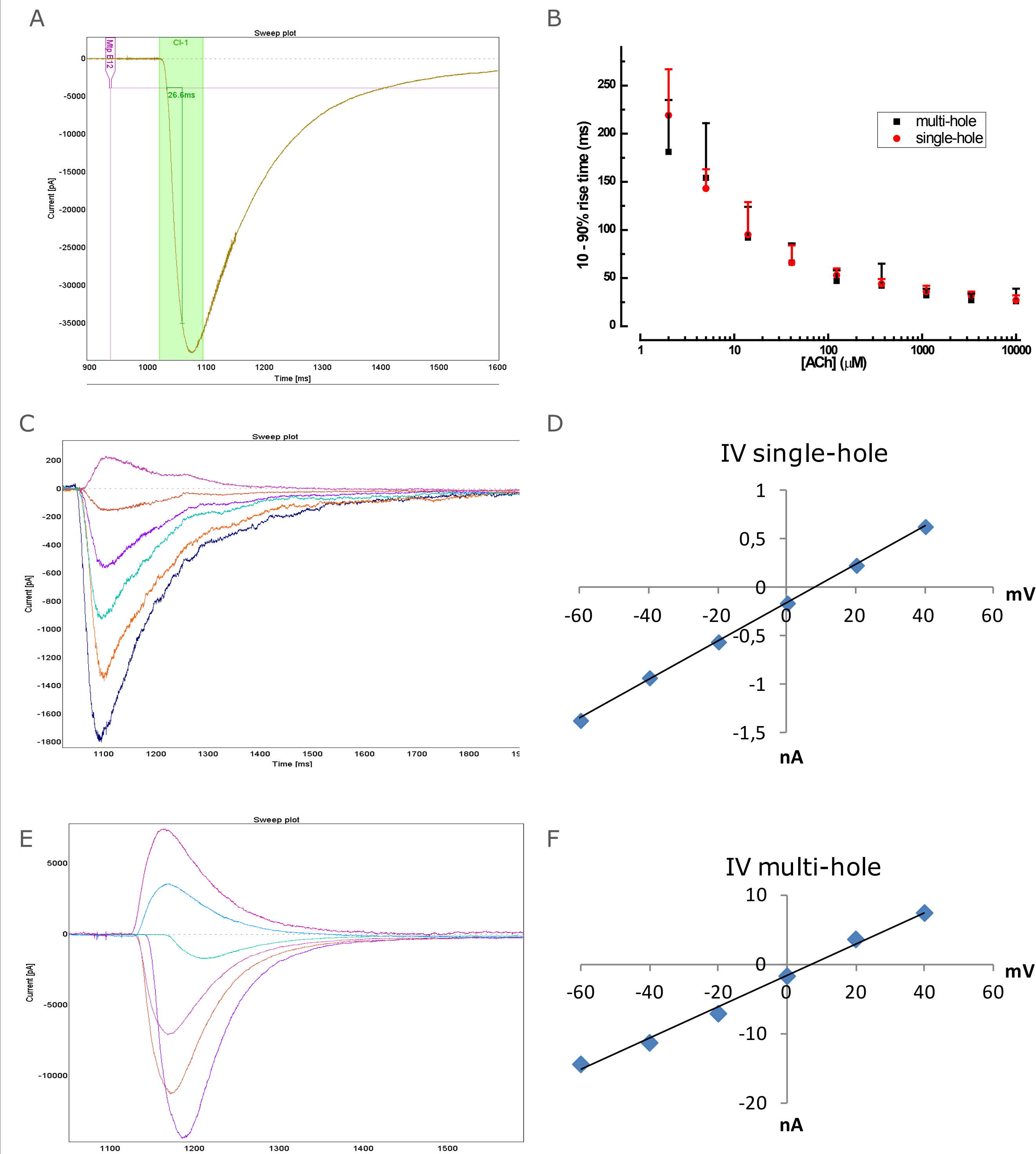
Ion channel	Compound	Single-hole	Multi-hole	Literature	Reference
nAChR $\alpha 1$	acetylcholine EC <sub>50</sub> ( $\mu$ M)	5.6	8.1	7.8	Shao et al 1998
	gallamine IC <sub>50</sub> ( $\mu$ M)	5.3	2.2	0.9	Paul et al 2002
ASIC1a	EC <sub>50</sub> (pH)	6.3	n/a	6.6	Li et al 2008
	amiloride IC <sub>50</sub> ( $\mu$ M)	25.2	33.0	3.4	Li et al 2008
GABA-A	GABA EC <sub>50</sub> ( $\mu$ M)	5.6	12.0	30.0	Feigenspan et al 2004
	Bicuculline IC <sub>50</sub> ( $\mu$ M)	1.2	1.5	1.7	Feigenspan et al 2004
	Glutamate EC <sub>50</sub> ( $\mu$ M)	236	344	631	Lerma et al 2001
GluR5	Kainate EC <sub>50</sub> ( $\mu$ M)	119	299	34	Lerma et al 2001
	CNQX IC <sub>50</sub> ( $\mu$ M)	1.9	2.7	0.92-6.1	Paternain et al, 1996

Table 1. Pharmacological data (IC and EC<sub>50</sub>) for all four ion channels, tested in multi-hole and single-hole mode.

% sites w current	single-hole	multi-hole
nAChR $\alpha 1$	90	93
ASIC1a	58	98
GABA-A	37	93
GluR5	65	91

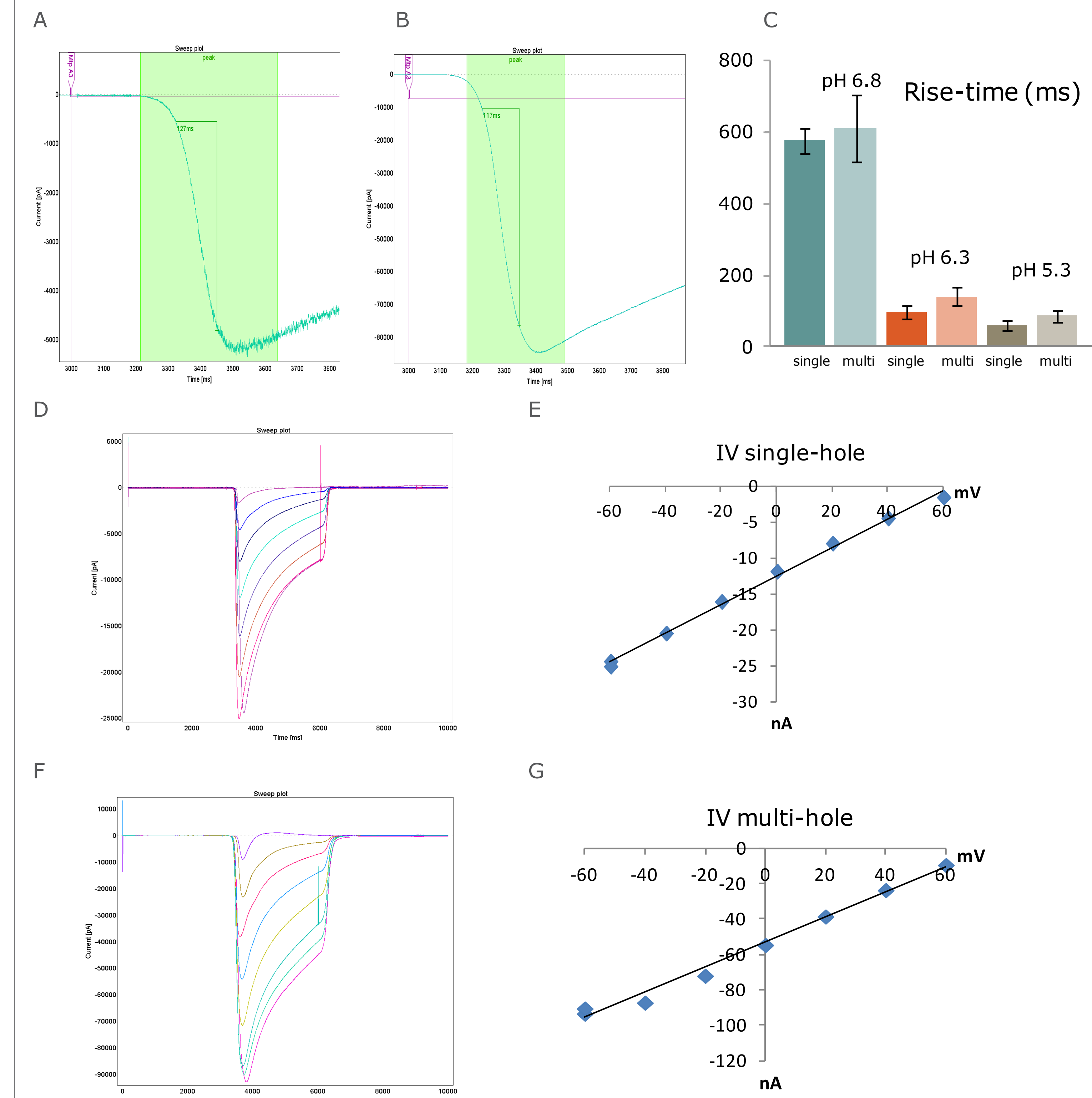
Table 2. Percentage of sites with usable current amplitude in single-hole versus multi-hole mode, for each respective cell-line.

Figure 2. nAChR  $\alpha 1$



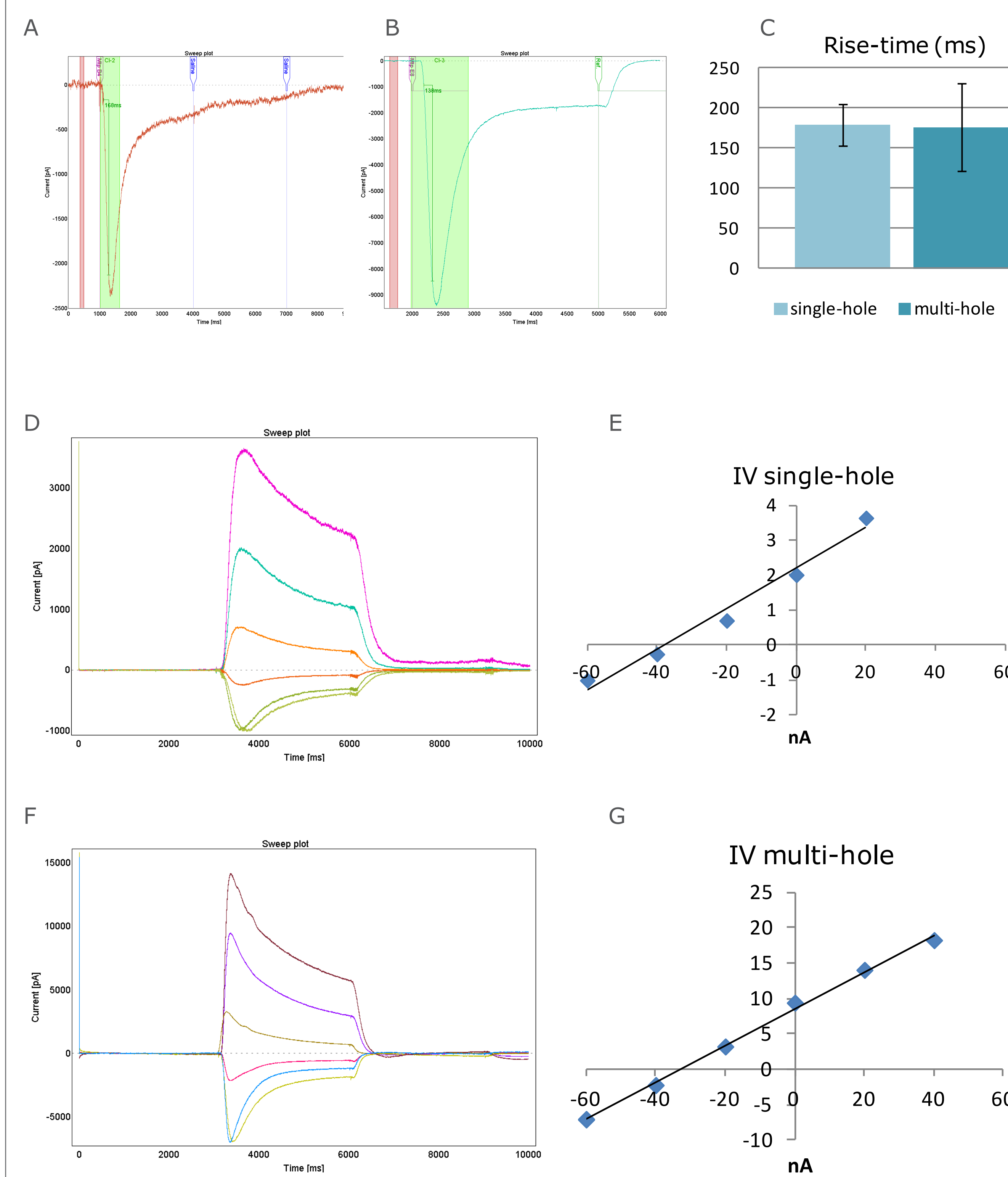
A: nAChR  $\alpha 1$  activated by 10 mM acetylcholine in a multi-hole experiment, showing the 10-90% rise time cursor.  
B: 10-90% rise-times (ms) for single-hole and multi-hole experiments at increasing concentrations of agonist (acetylcholine).  
C: Single-hole data example of nAChR $\alpha 1$  current activated with 100  $\mu$ M acetylcholine and recorded at holding potentials of -60, -40, -20, 0, 20, and 40 mV.  
D: Averaged single-hole I-V data. The calculated reversal potential, E<sub>rev</sub> = 8 ± 2 mV (n=5) (liquid junction potential corrected = -5 mV).  
E: Multi-hole data example of nAChR $\alpha 1$  current activated with 100  $\mu$ M acetylcholine and recorded at holding potentials of -60, -40, -20, 0, 20, and 40 mV.  
F: Averaged multi-hole I-V data. The calculated E<sub>rev</sub> = 8 ± 3 mV (n=11) (liquid junction corrected = -5 mV).

Figure 3. ASIC1a



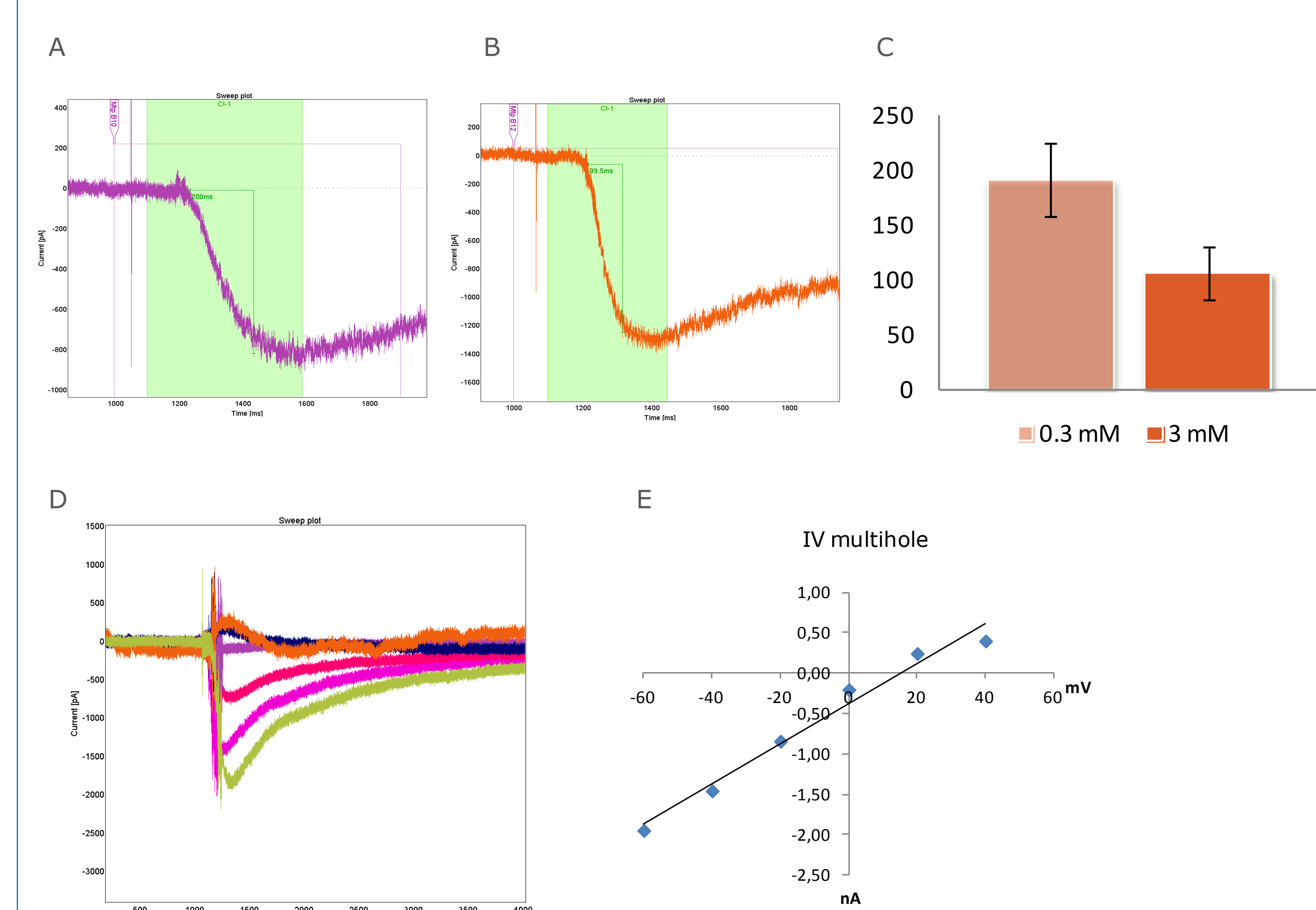
A: ASIC1a activated by pH 6.3 in a single-hole experiment, showing the 10-90% rise time cursor.  
B: ASIC1a activated by pH 6.3 in a multi-hole experiment, showing the 10-90% rise time cursor.  
C: 10-90% rise-times (ms) for single-hole and multi-hole experiments at increasing concentrations of agonist (pH 6.3).  
D: Single-hole data example of ASIC1a current activated at pH 6.3 and recorded at holding potentials of -60, -40, -20, 0, 20, 40 and 60 mV.  
E: Averaged single-hole I-V data. The calculated reversal potential, E<sub>rev</sub>(Na) = 67 ± 9 mV (n=4). The theoretical E<sub>rev</sub>(Na) for this Ringer's pair is 68 mV.  
F: Multi-hole data example of ASIC1a current activated at pH 6.3 and recorded at holding potentials of -60, -40, -20, 0, 20, 40, and 60 mV.  
G: Averaged multi-hole I-V data. The calculated E<sub>rev</sub>(Na) = 73 ± 4 mV (n=12).

Figure 4. GABA-A  $\alpha 1\beta 2\gamma 2$



A: GABA-A  $\alpha 1\beta 2\gamma 2$  stimulated with 12  $\mu$ M GABA in a single-hole experiment, showing the 10-90% rise time cursor.  
B: GABA-A  $\alpha 1\beta 2\gamma 2$  stimulated with 12  $\mu$ M GABA in a multi-hole experiment, showing the 10-90% rise time cursor.  
C: 10-90% rise-times (ms) for single-hole and multi-hole experiments at increasing concentrations of agonist (GABA).  
D: Single-hole data example of GABA current activated with 10  $\mu$ M GABA and recorded at holding potentials of -60, -40, -20, 0, 20, and 40 mV.  
E: Averaged single-hole I-V data. The calculated reversal potential, E<sub>rev</sub>(Cl) = -38 ± 4 mV (n=6) (liquid junction potential corrected -51 mV). The theoretical E<sub>rev</sub>(Cl) for this Ringer's pair is -51 mV.  
F: Multi-hole data example of current activated with 10  $\mu$ M GABA and recorded at holding potentials of -60, -40, -20, 0, 20, and 40 mV.  
G: Averaged multi-hole I-V data. The calculated E<sub>rev</sub>(Cl) = 37 ± 3 mV (n=10) (liquid junction potential corrected -50 mV).

Figure 5. GluR5



A: GluR5 activated by 0.3 mM kainate, in a multi-hole experiment, showing the 10-90% rise time cursor.  
B: GluR5 activated by 3 mM kainate, in a multi-hole experiment, showing the 10-90% rise time cursor.  
C: 10-90% rise-times (ms) for multi-hole experiments at two concentrations of kainate.  
D: Multi-hole data example of GluR5 current activated with 3 mM kainate and recorded at holding potentials of -60, -40, -20, 0, 20, and 40 mV.  
E: Averaged multi-hole I-V data. The calculated reversal potential, E<sub>rev</sub> = 16 ± 10 mV (n=14).

## Conclusion

QPatching in multi-hole mode with ligand-gated ion channels has a number advantages: 1) because it records the total current from ten cells patched in one recording unit, multi-hole mode allows measurements with cells exhibiting very small ion channel currents; 2) the gigaseal-based recordings provide a high signal-to-noise ratio giving efficient and accurate recordings; and 3) the flow channels ensure fast and reproducible liquid exchange around the cell giving very stable recordings after several compound additions. Our QPatch HTX data demonstrates the expected properties for these ligand-gated ion channels, when patched in multi-hole mode: The signal onset is the same as it is in single-hole mode and the pharmacological properties remain unaltered. QPatch HTX, with the higher success rate for sites with usable current thus provides an unprecedented combination of high throughput and high quality recordings.